Bulletin of the Seismological Society of America, Vol. 70, No. 4, pp. 999-1014, August 1980

EVALUATION OF *S* TO *P* AMPLITUDE RATIOS FOR DETERMINING FOCAL MECHANISMS FROM REGIONAL NETWORK OBSERVATIONS

BY CARL KISSLINGER

ABSTRACT

The ratios of the amplitudes of *SV* to *P*, as recorded on vertical component seismographs near the earthquake, provide a means of determining the focal mechanism. The observed ratios are compared with values calculated on the basis of dislocation theory, with the effects of transmission across boundaries and incidence on the free surface approximately accounted for by plane-wave coefficients. A search is made for the strike and dip of the fault that provides a fit to as many of the stations as possible, for the direction of fault slip assumed. The direction of slip may also be treated as a free parameter to be determined, but the theoretical results are especially simple for pure strike-slip or pure dip-slip faulting. The technique has been applied to the analysis of events in three settings, in which pure thrusting, pure strike-slip, and pure normal faulting could be assumed. The utility and the limitations of the method are illustrated by these examples. The important limitations are that the method cannot distinguish between conjugate mechanisms or show the sense of slip on the fault. It also has a weak resolution of strike for some commonly occurring mechanisms, so that the solution may depend on the readings at only a few stations.

The method has been used to pick out a group of foreshocks to an Aleutian Islands earthquake and to provide a focal mechanism for an event in the Rhine graben, at a place where such information is lacking and needed. A study of 15 central California earthquakes revealed no changes in fault plane orientation or in relative attenuation of *P* and *S* waves during 1 yr prior to a magnitude 5 earthquake.

INTRODUCTION

The determination of focal mechanisms of small to moderate earthquakes from the data gathered by regional networks is a basic tool in the investigation of local and regional scale tectonics. The number of stations is often limited, and in some regions of great interest, such as subduction zones, the azimuthal coverage is usually poor because the stations are all on one side of the active zone (Engdahl and Kisslinger, 1977).

Much more information about the source is present in the seismograms than that represented by the polarity of the first *P* arrival. Matching synthetic seismograms with observed ones is a powerful means of exploiting more of this information (see e.g., Helmberger and Burdick, 1979). Seismogram synthesis requires extensive computation and this approach is not yet developed to the point at which it is practical for the routine processing of large numbers of small events, especially for the high-frequency signals at short distances.

For a given velocity distribution, the amplitudes of the body waves observed at a particular azimuth and distance (equivalently, takeoff angle) are determined principally by the focal mechanism and depth, as pointed out by Lindh *et al.* (1978). The possibility of using the ratio of the maximum *S* amplitude to the maximum *P* amplitude as input to a procedure for determining focal mechanism has been tested as one way of extracting some of the additional information in the observed seismograms, without resorting to lengthy computations.

The ratio of the maximum amplitude of the vertical component of *SV* to the

maximum amplitude of the vertical component P, denoted $(SV/P)_z$, was chosen as the quantity to be observed. This choice was made because vertical-component instruments are widely used in regional networks, single instrument usage eliminates concern about accuracy of calibration, and SH or the horizontal component of SV, while perfectly feasible, requires rotation of components. This last is no problem if well-calibrated digital data are originally available. The use of amplitude ratios rather than absolute values of the amplitudes offers the advantage in general that, not only are problems of instrument calibration removed, but other factors affecting the recorded signal, such as transmission coefficients at boundaries, have a much smaller influence on the amplitude ratio than on the amplitudes of the two waves for cases that enter here. These effects are corrected for approximately in this study, but they are seen to be small.

$(SV/P)_z$ as observed at close distances should be independent of the magnitude of the earthquake. At larger distances, for which effects of inelastic attenuation are greater, changes in the ratio with magnitude may be expected because of differences in the dominant frequencies of the two wave types and the relative enrichment of low frequencies for larger events. No amplitude data from network seismograms for large earthquakes at small distances are available because of clipping, and the actual range of magnitudes for which the technique has been tested is small.

The selection of the amplitude to be read is a nontrivial problem, especially for the S wave. The intent here has been to read the peak-to-peak amplitude of the first or second half-cycle of P and S waves traveling directly upward from the hypocenter. Takeoff angles from the hypocenter solutions and travel-time curves are useful for determining if the first-arriving phase in the P and S groups are direct waves and for identifying arrivals at cross-over distances for various crustal paths. Some experiments with synthetic seismograms have demonstrated the problems caused by interfering arrivals, especially for S waves. Although head-wave arrivals can, in principle, be used as readily as direct waves, serious problems arise if the hypocenter is a short distance above a boundary between layers, so that direct and head waves interfere over the range of distances covered by the observations. This has proven to be a major problem for some deeper events in the Rhine graben.

After the hypocentral location has been calculated, the strike, dip, and direction of slip on the fault plane are determined by finding that combination which yields the best fit of the calculated amplitude ratios to those observed. In the cases presented to illustrate the method, the known regional tectonics and available first-motion data were such that it was judged acceptable to assume either pure strike-slip or pure dip-slip fault motion. The reliability of the solution thus obtained depends not only on the validity of this simplifying assumption, but also on the accuracy of the velocity model and the hypocentral location.

Some inherent limitations are that the method cannot choose between conjugate solutions, and it cannot distinguish the sense of slip, i.e., normal or reverse, left-lateral or right-lateral motion on a given plane. The latter problem is easily resolved by a few reliable first-motion polarities. A further limitation is that the resolution of fault strike for near-vertical strike-slip faults is weak and depends strongly on the availability of data from stations at particular azimuths for which the amplitude ratio is either very high or very low.

Theory

The expressions for wave amplitudes in an infinite medium generated by a point shear dislocation, derived by Vvedenskaya (1956) have been used to obtain equations for $(SV/P)_z$, as suggested by Feng (1974). Equivalent expressions are given by other

authors, e.g., Kanamori and Stewart (1976). One coordinate system is $\bar{x}$, $\bar{y}$, $\bar{z}$: $\bar{x}$ is parallel to the fault strike, such that when looking in the $+\bar{x}$ direction, the dip angle, δ, is positive downward to the right; $\bar{z}$ is positive downward. The takeoff angle, i_h, is measured upward from $\bar{z}$. $A = A_s - A_f$, where A_z is the azimuth to the station from the epicenter, and A_f is the fault strike, both referred to geographic coordinates; $\bar{y}$ makes a right-handed system.

These coordinates are related to the radial distance, r, the azimuth, A, and the takeoff angle by

$$\bar{x} = r \sin i_h \cos A, \bar{y} = r \sin i_h \sin A, \bar{z} = r \cos i_h.$$

The other coordinate system is x, y, z: y is the normal to the fault plane, chosen such that angle $(y, \bar{z}) = \delta$; z is parallel to the direction of slip of the fault block $y < 0$; x makes a right-handed system.

The angle $(z, \bar{x}) = \lambda$ is measured in the fault plane, positive clockwise about the $+y$ axis. Then

$$x = -\sin \lambda \bar{x} + \cos \delta \cos \lambda \bar{y} + \cos \lambda \sin \delta \bar{z}$$

$$y = -\sin \delta \bar{y} + \cos \delta \bar{z}$$

$$z = \cos \lambda \bar{x} + \sin \lambda \cos \delta \bar{y} + \sin \lambda \sin \delta \bar{z}.$$

The far-field wave amplitudes in an infinite, homogeneous, elastic medium (Vvedenskaya, 1956) are

$$u_{sv} = \frac{\mu ba[-2yz \cos^2 i_h + \bar{z}(z \cos (y, \bar{z}) + y \cos(z, \bar{z}))]}{\pi \rho V_s^2 r^2 \sqrt{r^2 - y^2} \sin i_h \cos i_h}$$

$$u_p = -\frac{\mu bayz}{\pi \rho V_p^2 r^2 \sqrt{r^2 - y^2}}$$

where μ, shear modulus; b, amount of slip across the dislocation; a, radius of the dislocation; ρ, density; V_p, V_s, the two body-wave velocities. The time dependence has been omitted.

Thus, the ratio of the wave amplitudes as they leave the source is

$$(SV/P)_0 = (V_p/V_s)^2 \left[2 - \frac{r}{yz \cos i_h} (y \cos (z, \bar{z}) + z \cos (y, \bar{z})) \right] cot\ i_h.$$

In terms of δ, A, λ

$$(SV/P)_0 = \left(\frac{V_p}{V_s}\right)^2 cot\ i_h$$

$$\left[2 - \frac{(cot\ \delta - \tan \delta)\sin \lambda \tan i_h \sin A + 2 \sin \lambda + csc\ \delta \cos \lambda \tan i_h \cos A}{D} \right] \quad (1)$$

where

$$D = \cos \lambda \cos A \sin i_h[-\sin i_h \sin A\ sec\ \delta + \cos i_h\ csc\ \delta]$$

$$+ \sin \lambda \sin i_h \cos i_h \sin A(cot\ \delta - \tan \delta) + \sin \lambda(\cos^2 i_h - \sin^2 i_h \sin^2 A).$$

For a normal fault, $\lambda = 90°$, for a reverse fault, $-90°$. $\lambda = 0°$ for left-lateral strike-slip and 180° for right lateral. The ratio is seen to be insensitive to the direction of slip, as expected, since the polarities of both waves are reversed if the sense of motion is reversed.

The simple cases of pure strike-or dip-slip are used in this work. For the former

$$(SV/P)_0 = \left(\frac{V_p}{V_s}\right)^2 cot\, i_h \left[2 - \frac{1}{\cos^2 i_h - \sin i_h \cos i_h \sin A \tan \delta}\right]. \tag{2}$$

For a perfectly vertical strike-slip fault

$$(SV/P)_0 = 2\left(\frac{V_p}{V_s}\right)^2 cot\, i_h \tag{3}$$

so that azimuth drops out. This simplification motivated the test of the use of $(SV/P)_z$ as a way of detecting temporal changes of relative attenuation of P and S waves for earthquakes on the San Andreas Fault. From (2), the observed quantity is not very sensitive to the strike of a near vertical strike-slip fault. For dip-slip faulting,

$$(SV/P)_0 = \left(\frac{V_p}{V_s}\right)^2 cot\, i_h \left[2 - \frac{2 + (cot\, \delta - \tan \delta)\tan i_h \sin A}{\cos^2 i_h - \sin^2 i_h \sin^2 A + \sin i_h \cos i_h \sin A (cot\, \delta - \tan \delta)}\right]. \tag{4}$$

The use of these expressions in the search for the strike and dip that fit the data best is facilitated by the recognition of combinations of values of the angles for which u_{sv} or u_p goes to zero. These results have been used for a long time in focal mechanism studies (e.g., Stauder, 1962). For the dip-slip case, $(SV/P)_0 = 0$ for

$$\sin^2 A - 2\, cot 2\delta cot 2i_h \sin A + 1 = 0.$$

As an equation for A, there is a double root, $\sin A = \pm 1$ for $\tan 2\delta = \pm cot 2i_h$. The relevant values are

$$A = 90° \quad \text{for} \quad \delta = 135° - i_h$$
$$A = 270° \quad \text{for} \quad \delta = i_h - 45°, \delta \neq 45°.$$

For dip-slip, $(SV/P)_0 \to \infty$ $(u_p = 0)$ for

$$\sin^2 A - 2 cot 2\delta cot i_h \sin A - cot^2 i_h = 0.$$

For $\delta = 45°$, $\sin A = \pm cot\, i_h$.

The corresponding values for strike-slip faulting are

$$(SV/P)_0 = 0 \quad \text{for} \quad \sin A = cot\, 2i_h cot \delta.$$
$$(SV/P)_0 \to \infty \quad \text{for} \quad \sin A = cot i_h cot \delta.$$

The amplitude ratios given by (1), (2), or (4) must still be propagated through the velocity structure to the free surface and converted to the ratio of vertical components, as recorded. Uncertainties in the structure will adversely affect the results, and this is a difficult problem on the local scale of the observations used here, for complex settings like Adak Island and the San Andreas Fault. With the angle of incidence at the surface calculated for each i_h, the results of Gutenberg (1944) for plane waves are used as an adequate approximation to W_p and W_{sv}, the ratios of the vertical component of P at the surface to the incident amplitude (P_z/P_0) and the vertical component of SV at the surface to the incident amplitude (SV_z/SV_0). The observed quantity is given by

$$(SV/P)_z = (SV/P)_0 \frac{W_{sv}}{W_p}. \tag{5}$$

For $V_p/V_s = 1.732$, W_{sv}/W_p varies between 0.996 and 1.155 for angles of incidence at the surface between 37° and 80°, so that the free-surface effect on the amplitude ratio is small and easily accounted for. These angles are greater than the critical angle for SV to P conversion by reflection, so that W_{sv} is complex. The correction for the free surface effect is a major difficulty for incidence angles between about 32° and 36°, the range around the critical angle within which W_{sv} changes rapidly for small changes in the angle.

For all three cases investigated, the structure used to locate the events, for stations at the small epicentral distances used, consisted of a single layer over a thick layer, with the focus in the lower layer. The ratio of the transmission coefficients at the boundary is close to 1 for all of the cases and was taken as such.

The properties of $(SV/P)_z$ as a function of azimuth, from (5), for the cases expressed by (2) and (4) are illustrated for representative values of dip, δ, in Figures 1 and 2. *Log* $(SV/P)_z$ is used throughout this work. The poor resolution of strike for dips near 90° is seen in Figure 1. Most of a set of observations at stations distributed randomly in azimuth will be close to the same value (for the same distance). This value depends on the dip. Only if there happen to be stations at azimuths at which observed $(SV/P)_z$ is either high or low, can the fault strike be fixed. In practice, this implies that the solution for the strike will often depend on readings at only a few stations. The situation is similar for dip-slip, (Figure 2), for dips near 45°.

Adak Island Foreshocks

The first application of these principles was to a group of small earthquakes in a tightly clustered active zone near Adak Island, Alaska. The details of the network, the seismicity, and the results of the experiment are given in Engdahl and Kisslinger (1977).

During an attempt to establish P and S body-wave magnitude scales for these earthquakes, based on observations at the permanent observatory ADK, it was noted that some events fell far off the log amplitude-duration magnitude line that fit most of the data. When log $(SV/P)_z$, as observed on the Benioff vertical at ADK, was examined for the set of 37 events, it was seen that, although most had a value of this parameter of about 0.7 [$(SV/P)_z = 5$], a small group had values ranging from 1.3 to infinity (P too small to read). Some of these anomalous events were spatially grouped on the epicenter map and appear to be associated with a distinct minor structure. It was noted that four of these were grouped in time, occurring in a

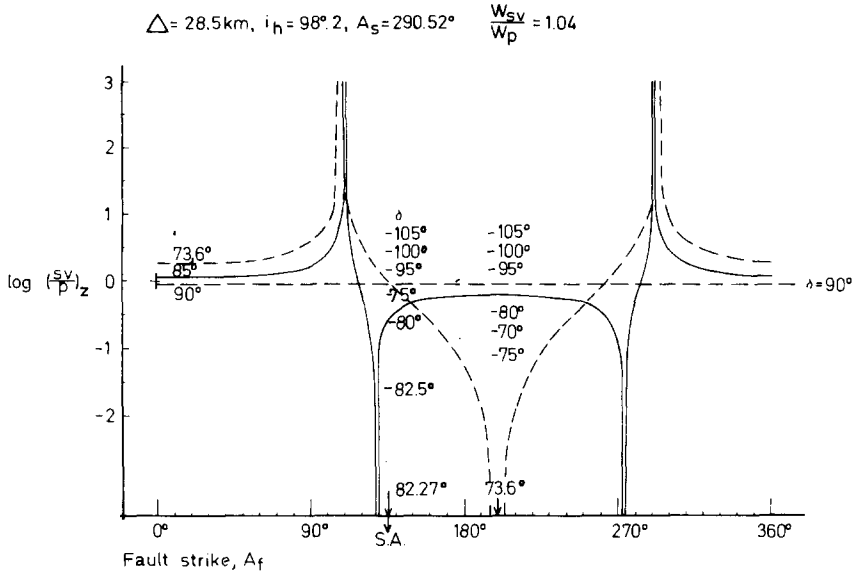

FIG. 1. Theoretical log $(SV/P)_z$ as a function of fault strike for a pure strike-slip fault and dips of 73.6°, 85°, and 90°, for a typical station near Bear Valley, California (SRS). S.A. marks the surface strike of the San Andreas Fault. The short dashes mark the values of log $(SV/P)_z$ for two values of the strike, for various other dips.

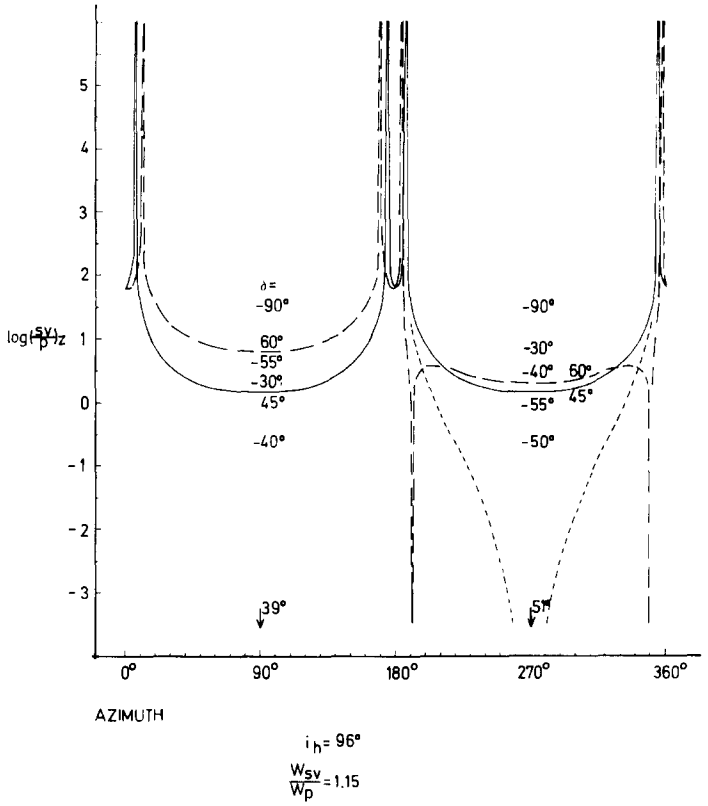

Fig. 2. Theoretical log $(SV/P)_z$ as a function of azimuth for a pure dip-slip fault and dips of 45° and 60°. Azimuth = $A_s - A_f$, the station azimuth from the epicenter minus the fault strike. The short dashes mark the values of log $(SV/P)_z$ for various other dips.

sequence following $3\frac{1}{2}$ months of quiescence in this usually active zone, just preceding a magnitude 5 earthquake. When these events were examined in detail, it was seen that their focal mechanisms, as indicated by the detection of compressional first motions at a few of the easternmost stations, were different from the usual events, for which dilatations are seen at all of the local stations. This and other criteria led to the conclusion that these events were true foreshocks of the magnitude 5 earthquake, as discussed in Engdahl and Kisslinger (1977).

Equations (4) and (5) were used to calculate the value of log $(SV/P)_z$ at ADK for a pure thrust fault. A strike of 260°, parallel to the trend of the island arc, from conventional first-motion analysis and a dip of 45°, predicts a value of 0.75, in good agreement with the most frequently observed values near 0.7. A strike of 222°, normal to the direction of relative plate motion, with a dip of 39°, gives the same value. For a strike of 195°, consistent with the foreshock first-motion distribution, a dip of 45° yields a value for a log $(SV/P)_z$ of 4 (ADK is very near a nodal plane), concordant with the large values observed for the foreshocks. If the strike of 260° is taken as the fault orientation for the background seismicity, based on first-motions, the conclusion is that the fault planes of the foreshocks had rotated 65° from the usual orientation, without appreciable change of dip.

The significance of this example is that routine observations of $(SV/P)_z$ at one well-placed station identified for further study a group of earthquakes with interesting source properties, without the need for fault plane solutions for all of the numerous events. No claim is made, of course, that an independent fault plane solution can be derived from observations at one station.

Chin *et al.* (1976) observed $(SV/P)_z$ for 15 foreshocks of the Haicheng earthquake (February 4, 1975) at 12 regional stations. They found that, except for clipping for the larger events, the ratios at each station were stable, concordant with an almost constant fault plane orientation and slip direction for all of these events. They did not present data for background seismicity prior to the foreshocks, but did show that the amplitude ratios for the aftershocks were widely scattered at any one station.

Bear Valley, California Earthquakes

The useful result at Adak and the potential applicability of $(SV/P)_z$ to prediction (Feng, 1974; Lindh *et al.*, 1978) called for a more thorough test of the technique. Because the mechanisms on the central San Andreas Fault are all almost certainly strike-slip on a nearly vertical plane, a set of events in this region was selected for study. The many uncertainties of focal mechanisms and velocity structure in the Adak subduction zone could be avoided and the range of credible solutions sharply restricted.

Fifteen small events that occurred near Bear Valley, California between January 6, 1971 and February 15, 1972 were selected for analysis. Eleven of these were tightly clustered between 36° 33.5′ to 36° 38′N, 121° 10′ to 121° 15′W, near the site of a magnitude 5.0 earthquake on February 24, 1972 and much subsequent activity (Ellsworth, 1975). Precursory changes associated with the approach of the large event could be sought. Three other events were just southeast of this cluster, also on the San Andreas Fault, and one was off the fault to the northeast.

Precursory changes of the velocity ratio, V_p/V_s, have not been detected in central California (McEvilly and Johnson, 1974). On the other hand, McNally and McEvilly (1977) interpreted a reduction in the amount of distortion of the P nodal planes of

earthquakes in the same place studied here, after the February 24, 1972 earthquake, as evidence of a reduction in the lateral velocity contrast across the fault, at the depths of the earthquakes, as a result of the earthquake. They detected the maximum amount of nodal plane distortion seen anywhere along this segment of the San Andreas Fault at the site and during the time of occurrence of the earthquakes used in this study. This evidence, as well as the results of Engdahl and Lee (1976), indicates that there may be difficulties in the straightforward application of this technique based on the assumption of horizontal plane layers. Refraction at vertical boundaries will introduce errors in the determination of the point on the focal sphere from which a ray left on its way to a particular station.

Other conceivable seismological precursors are changes in focal mechanisms that would be revealed by changes in $(SV/P)_z$ with time at individual stations, and changes in the distance dependence of $(SV/P)_z$ because of changes in the relative inelastic attenuation of the two body waves. The theory of O'Connell and Budiansky (1977) suggests that Q_s for shear waves will be sharply reduced relative to Q_p for P waves at some frequencies if dilatancy occurs in a fluid-saturated rock. Although dilatancy would not be revealed by changes in V_p/V_s if the rock remains continuously saturated, in principle it might be detected as changes in relative attenuation. Feng (1974) interprets his data as revealing attenuation changes.

Usable data were severely limited by the small dynamic range of the instrumentation and the overlapping of traces on the multi-channel film records. An example of a typical seismogram is shown in Figure 3. The best data came from events in the range M 1.3 to 1.8. Data were limited to distances of about 65 km to avoid complications due to head-wave arrivals. The greatest uncertainty was the selection of the small S wave at the larger distances. In some cases, this was done on the basis of the expected arrival time only, and then a notation was made that the amplitude read was an upper bound on the true S amplitude.

For each earthquake, log $(SV/P)_z$ was plotted against distance, and compared with the curve, from equations (3) and (5) for a vertical strike-slip fault at the depth of the earthquake, as given in the USGS catalog (Wesson *et al.*, 1972). As seen in the examples in Figure 4, this curve follows the trend of the data and in most cases, lies within the range of values defined by the data without empirical curve-fitting of any kind. The basic theory, assuming perfect elasticity, does seem to describe the general behavior. However, some points, including some that were judged to be highly reliable, fall far from the theoretical curve (especially true since a logarithmic scale is used).

A search was made for a focal mechanism that would satisfy all of the data. A small range of strikes about the orientation of the surface trace of the San Andreas Fault, 138° was used, and the two values of dip that yielded observed value of $(SV/P)_z$ were calculated for each station. For almost every station for every earthquake, agreement was found for a dip within 5° of vertical for the strike of 138°. The mean and standard deviation of the dips so determined are given in Figure 4 and Table 1. McNally and McEvilly (1977) found from analyses of first motions for a large number of earthquakes spanning the time interval involved here that, earthquakes on this part of the San Andreas Fault were all characterized by strike-slip motion on a vertical plane, with strikes uniformly within 1° and 2° of the value used here.

The events selected for Figure 4 cover the range of depths, 3.6 to 11.8 km, and illustrate several important points that emerged. In Figure 4a, the event with the shallowest reported depth that was studied yields a mean dip near 90°, but with a large standard deviation of 9°. The curve for a vertical fault at 3.6-km depth passes

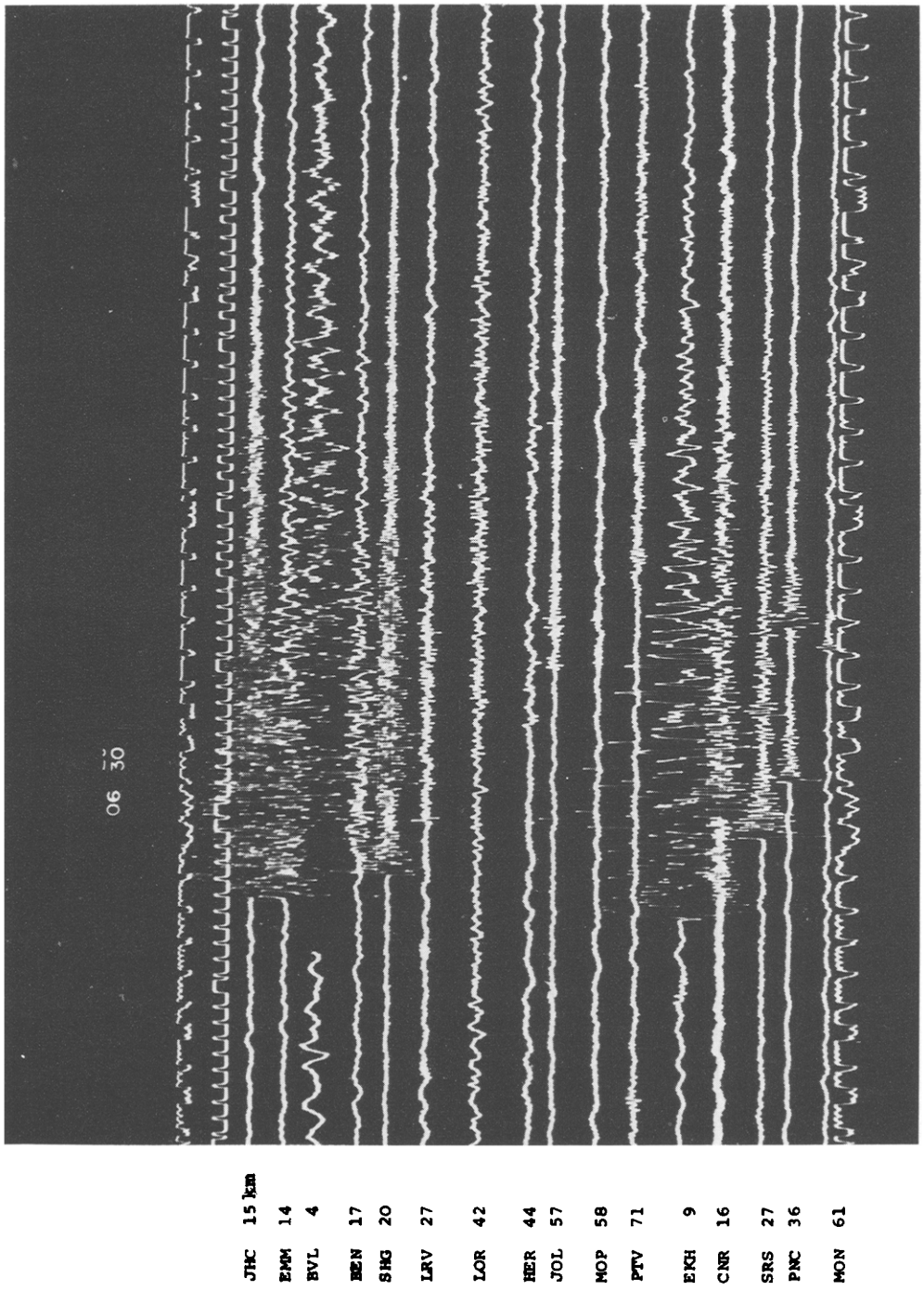

FIG. 3. Typical seismogram for a Bear Valley earthquake, event of February 15, 1972 (06:29); M, 1.3; h, 5.1 km.

below all of the data points except one (EKH). If the depth is arbitrarily taken as 6 km, a frequent depth for events at this site; the curve goes through the data, and the scatter of the best-fitting dips is greatly reduced to ±5.2°. If the true depth is near 6 km, the ray from the focus to EKH is incident at the surface at very close to the critical angle for SV to P reflection, so that the poor fit of EKH may be thus explained.

Figure 4b shows a typical, well-behaved event. Again, EKH has a near-critical angle of incidence and is the only station that cannot be fitted with a dip near 90°. The mean dip shown does not include the value for EKH.

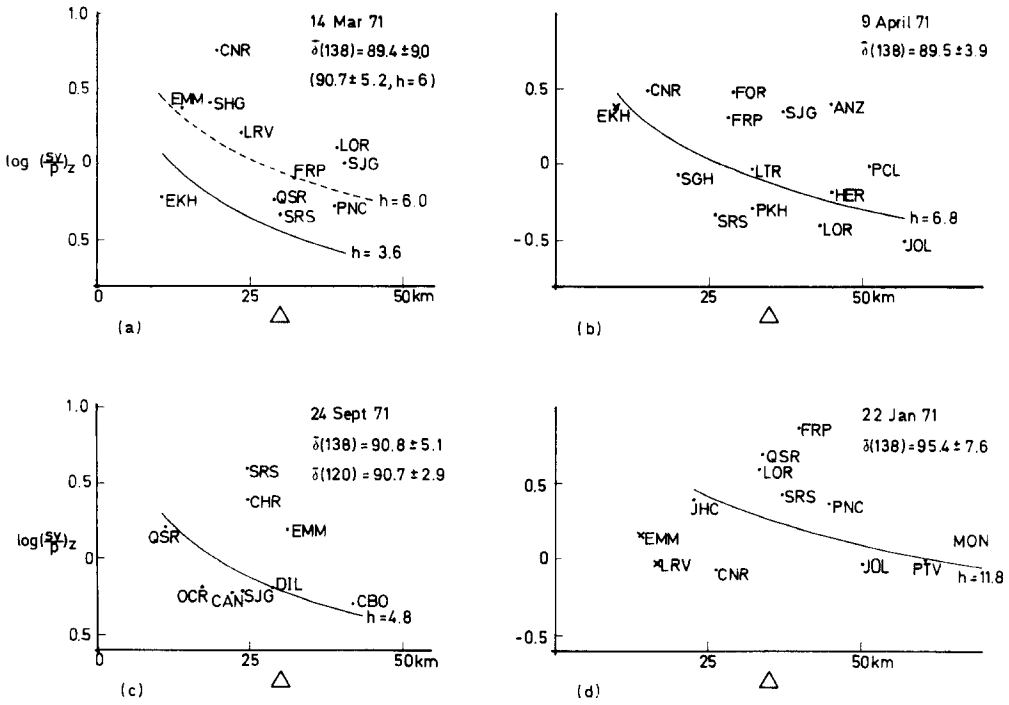

FIG. 4. Data $(SV/P)_z$ for selected central California events. The solid curve is the theoretical log (SV/P) versus distance relation for a vertical strike-slip fault at the indicated depth. $\bar{\delta}(138)$ is the mean of the dips fitting the observation at each station for a fault strike 138°. × denotes stations at which the angle of incidence at the surface is close to the critical value for SV to P reflection.

The event in 4c is the only one for which a complete search through fault azimuth and dip was made. The event is about 14 km from the San Andreas Fault, on the northeast side, some 36 km from the Bear Valley cluster. The mean dip for a fault parallel to the San Andreas is 90.8 ± 5.1°, with station SRS deleted. The best fit is a dip 90.7 ± 2.9°, with a strike of 120°. This difference in strike cannot be taken as significant because it is controlled by only two stations, CHR and EMM. Six of the stations have at least one solution close to 90° for all strikes tested, illustrating the poor resolution mentioned above. Clearly, the mean dip will always be close to 90° because practically all of the stations fall close to the curve for that dip in Figure 4c.

Only station SRS cannot be satisfied by a solution with a southeast strike and dip near vertical. The best solution that fits SRS is strike 210°, dip 76.1 ± 8.2°. This solution rejects station CHR and has more scatter than the one above. For almost every event, one or two stations did not fit the best solution. However, these were

not always the same stations and the explanation given is probably just bad data, especially bad picks of S. Other factors do enter in principle, e.g., local surface structure and known lateral velocity variations (Engdahl and Lee, 1976; McNally and McEvilly, 1977). Some preliminary attempts to incorporate these factors were made. The use of local structure at the station rather than the average structure did reduce some discrepancies. The full investigation of the effects of lateral velocity variations is a subject for future work.

Figure 4d is for the deepest event studied. Here, the two closest stations, EMM and LRV, have incidence angles close to critical and the surface correction applied did not result in any reasonable solutions. This event gave the greatest departure from a vertical fault, 84.6° to the northeast, but this difference of 5.4° is not significant.

TABLE 1

MEAN DIP FOR CENTRAL CALIFORNIA EARTHQUAKES*

Date (Time)	M	h (km)	δ° (138)	N	
1971					
06 Jan. (00:37)	1.3	4.5	90.7 ± 2.2	9	
21 Jan. (19:40)	1.8	6.3	93.9 ± 8.6	8	Also 100 ± 7.8
22 Jan. (05:46)	1.1	5.9	95.0 ± 7.8	6	Also 98.9 ± 7.3. Southeast of cluster
22 Jan. (12:05)	1.0	11.8	95.4 ± 7.6	11	Southeast of cluster
14 Mar. (18:13)	1.1	3.6	89.4 ± 9.0	9	90.7 ± 5.2 if h is changed to 6 km
09 Apr. (09:10)	1.3	6.8	89.5 ± 3.9	13	
13 May (15:28)	1.8	6.7	87.9 ± 4.9	9	
14 May (10:59)	1.4	5.4	90.1 ± 3.4	13	
24 Sep. (06:59)	1.0	4.8	90.8 ± 5.1	8	Northeast of San Andreas. Best fit: $A_f = 120$, $\delta = 90.7 \pm 2.9$
1972					
26 Jan. (17:30)	1.9	5.9	89.6 ± 2.9	13	
30 Jan. (16:06)	1.7	6.2	88.6 ± 3.8	17	Local thickness for upper layer gives 87.6 ± 4.1
31 Jan. (09:22)	1.4	4.2	91.6 ± 4.8	12	
15 Feb. (06:29)	1.3	5.1	89.4 ± 4.9	11	
15 Feb. (09:18)	1.0	11.1	90.6 ± 3.8	7	Southeast of cluster

* Pure strike-slip fault parallel to the surface trace of the San Andreas (dip measured down to southwest; N is number of stations in the mean).

The Bear Valley results are summarized in Table 1. The mean of the dips closer to 90° calculated for each station for a fault strike of 138° is listed. The dip values farther from 90° tended to disagree widely among themselves and not define a solution for most events. However, for two cases listed, the second solution is as good as the near-vertical one in terms of scatter.

These results do not contradict those of Engdahl and Lee (1976), who found large departures from verticality. They are subject to the same errors caused by lateral velocity variations as conventional fault plane solution, and only raytracing through the structure, to get the correct azimuth and takeoff angle, can lead to solutions directly comparable to theirs. Their velocity model for the southwest side of the

fault was used for one event, but no improvement in terms of reduced scatter of dips or reconcilation of stations in strong disagreement resulted.

Darmstadt, Germany Earthquake (June 7, 1979)

A small earthquake, coda duration magnitude 2.3, occurred in the northern part of the upper Rhine graben, near Darmstadt, on June 7, 1979, 00:45:16:35 UTC, at 49° 54.5'N, 8° 39.5'E, depth of 5.9 km (K.-P. Bonjer, personal communication). Only a few focal mechanisms of uncertain quality have been obtained for the general region and none for events within this part of the Rhine graben itself. This active zone is important for understanding the contemporary state of stress and the seismotectonics of central Europe. The regional seismographic observations of this earthquake were good, covering distances of 18 to 230 km with adequate azimuthal distribution. However, the number of reliable first-motion directions was insufficient to define a good fault plane solution, so an opportunity was offered to try the technique using amplitude ratios on an event of some importance.

$(SV/P)_z$ was determined from the seismograms at distances less than 100 km to avoid interference from crustal reflections or P_n. The seismograms, shown in Figure 5, are from the permanent and mobile stations of the Karlsruhe University network, except for WDB, which is operated by the University of Frankfurt. The epicentral distance and azimuth to each station is given on the figure. The original time scales are either 240 mm/min (ROS and TRO) or 120 mm/min. An aftershock, 30 min 28 sec after the main shock, is seen on most of the records. The S wave is clipped at ROS and WDB. Because the aftershock appears to be in the same place, with a similar mechanism, as the main shock, $(SV/P)_z$ for this event was read for ROS and used in the procedure, although not given very much weight. Station DON has a clear second P arrival, a crustal reflection, and from KLT to greater distances, the P phases are indistinct and complex.

Pure dip-slip faulting was assumed for the analysis so equations (4) and (5) were used, with the velocity structure for the Rhine graben worked out by the Geophysical Institute, Karlsruhe University. Angles of incidence at the surface were 60° to 65°. The dip yielding the observed amplitude ratio was calculated for each station for strikes between 270° and 90°. The remaining 180° of strikes are the conjugate solutions to those calculated. Two values of dip are found for each $(SV/P)_z$ and strike. A graph of these dips versus fault strike was examined for points of convergence at which a large number of the stations were simultaneously satisfied. Two such points were seen

$$A_f = 20°,\ \bar{\delta} = 51.6 \pm 5.1°; \quad \text{and} \quad A_f = 313°,\ \bar{\delta} = 45.4 \pm 1.0°.$$

The first of these is roughly parallel to the nearby eastern boundary fault of the Rhine graben and seemed a likely candidate. However, from the data alone, the second solution is strongly preferred. It satisfies every station for which the data were originally annotated as reliable, with a small scatter of the dip. The value given above does not include the aftershock reading at ROS. If this reading is retained as a datum, it fits quite well, yielding a mean dip, 46.7 ± 3.9°. The strike of this solution is controlled by TRO and CAM, which converge only at this point. WDB also fits, in the general sense that the predicted S amplitude, eight times P, looks very reasonable in terms of the actual seismogram, Figure 5. The more distant stations, KRA, KOE, and PET do not fit this solution and will be discussed later. The fault described by this solution is roughly parallel to the Darmstadt-Gross Gerau-Mainz epicenter lineation discussed by Landsberg (1931).

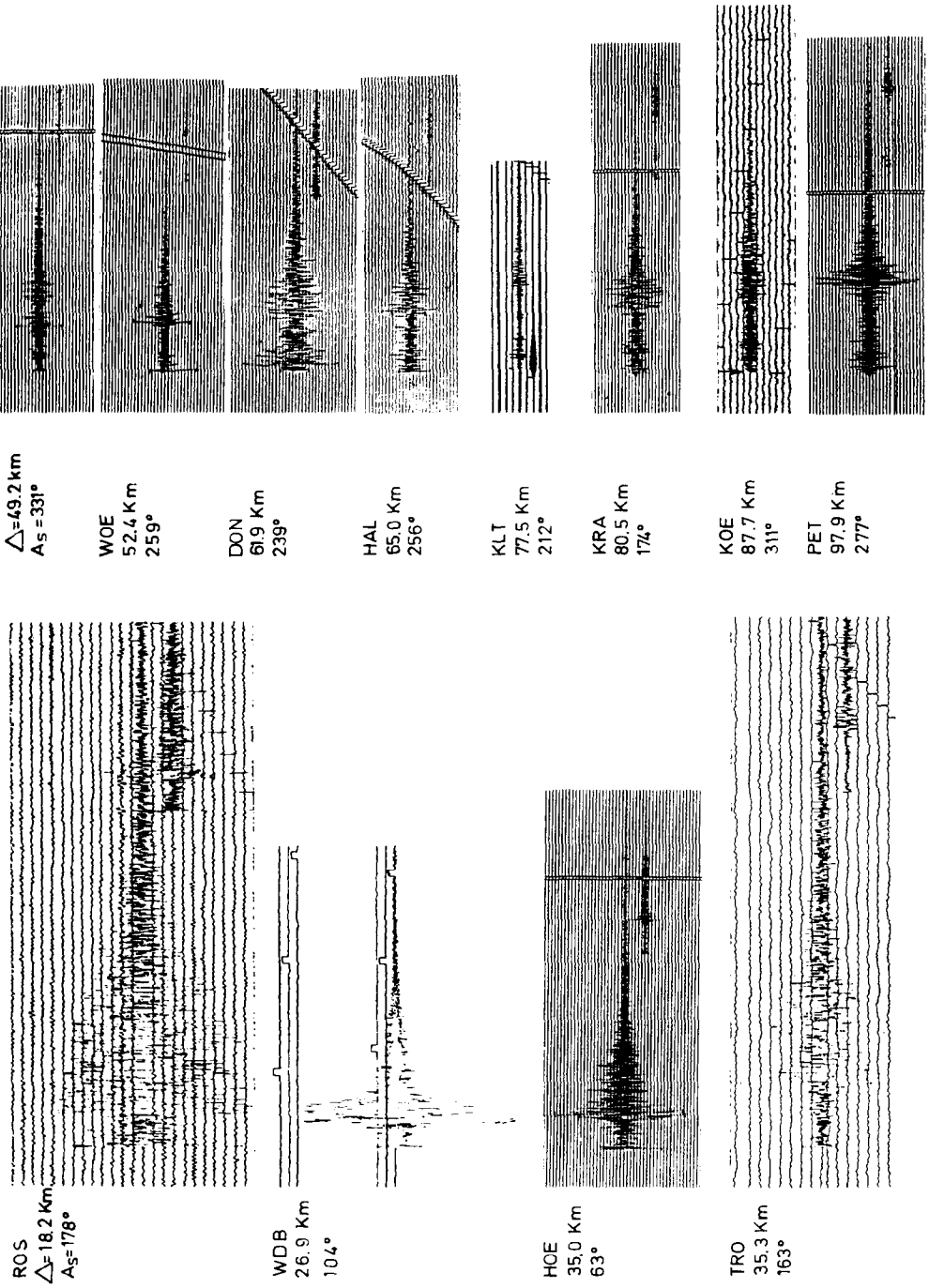

FIG. 5. The seismograms from the Darmstadt earthquake.

The roughly north-south solution is not as good a fit. The mean dip given above is for the eight best-fitting stations, and some good data are excluded from it. Of the three stations that do not fit the northwest striking solution, only KRA fits this one. However, the seismogram from ROS, Figure 5, even though clipped, appears to rule out this solution, which puts a nodal line for P through this station.

The three stations that do not fit the preferred solution all have emergent P phases. KOE is on a node for this solution, so an unreliable P is not surprising. PET is more of a concern because the weak P relative to S is not concordant with the solution, which calls for a vertical SV amplitude 0.6 the vertical P amplitude. The weak P arrival may be the effect of transmission across the sharp vertical boundary between focus and station formed by the deep-going south border fault of the Hunsruck Mountains (suggested by Bonjer, personal communication). The first-motion data compiled by Bonjer, while insufficient to define a reliable solution, are consistent with this one and show the sense of slip to be normal faulting.

Many earthquakes in and near the Rhine graben have strike-slip displacements. The theoretical curve of log $(SV/P)_z$ versus distance for a vertical strike-slip fault at a depth of 5.9 km falls below all of the data from this earthquake except station DON and the aftershock value at ROS. Depths of 10 to 15 km yield curves that come near the observed values, but the calculated depth seems constrained well enough to eliminate a shift of this account. In addition, the reliable first-motion directions are not compatible with a large strike-slip component of fault slip.

Further Experiments

This method of determining focal mechanisms has been further developed by testing a practical technique for making λ, the slip direction, a free parameter. This has been accomplished by applying iterative least-squares adjustments to the three variables, dip, strike, and slip. The available first-motion polarities are examined to determine if the mechanism appears to be dominantly strike-slip or dip-slip and to set limits on acceptable dips and strikes if possible. A starting solution is found by determining the best-fitting pure strike-slip or dip-slip fault, in the manner described for the test cases above. The derivatives of log $(SV/P)_z$ with respect to dip, strike, and slip are then calculated for the neighborhood of this solution. Adjustments to the three parameters are then calculated in the usual way by minimizing the sum of the squares of the differences between the observed and calculated values of log $(SV/P)_z$, taken as a linear function of the three parameters.

This approach has been tested on a few small Rhine graben events for which the local networks produced about six good seismograms with a good azimuthal distribution. The process converged quickly for these cases. For one case, a strike-slip event with a small dip-slip component, a test was made to learn if the solution had converged to a local minimum. A pure dip-slip solution was taken as the start of the procedure, and by the second iteration the strike-slip nature of the mechanism emerged.

Applicability to Prediction

If the fault planes of small events change orientation during the time prior to a large earthquake, this behavior will be detectable by observations of $(SV/P)_z$, as fully discussed by Lindh *et al.* (1978). The Adak experience shows that, if small events in a tightly concentrated source are observed over a long period of time at a good station, in a region characterized by a dominant focal mechanism, signals at that one station are sufficient to detect fault plane rotations.

No significant changes in the orientation of the Bear Valley fault planes during the year before the February 24, 1972 earthquake were revealed by the small sample of events selected as representing this time. Although more events should be studied before generalizing to a conclusion that no unusual focal mechanisms occurred, the failure to find precursory rotations of the fault planes is in general agreement with the results of Warren (1979) for the Hollister area.

No changes with time of the inelastic attenuation are required by the California data. The falloff of the amplitude ratio with distance does raise some perplexing questions about the Q values involved. The data are satisfied by theory for infinite Q, but because we are dealing with amplitude ratios, the data will also be satisfied if f/VQ is the same for P and S waves. VQ is expected to be about four times as great for P waves as S ($1.73 \times 9/4$), so the data are accounted for if P frequencies are about four times S frequencies. For some of the stations, this is roughly satisfied, with P having a frequency of about 10 Hz and S about 3 Hz. At many stations, however, the two frequencies seem to be almost the same by inspection of the seismograms, yet the SV amplitudes at these stations are not small as would be expected. Bakun and Bufe (1975) showed that S waves are strongly attenuated while propagating along the fault zone, for signals peaking at 2 and 3 Hz. It is not known to what extent these low Q's apply outside of the fault zone itself or to higher frequency signals.

The analysis of attenuation is further complicated by the fact that a substantial part of the energy loss from the waves at the high frequencies involved must be due to scattering in the inhomogeneous crust. The entire question of the implications of these results for attenuation should be explored by application of the same analysis to digital data, far better suited to spectral analysis than the analog records used here.

Feng's (1974) interpretation of his data as revealing attenuation changes depends strongly on his assumption that the events he was analyzing had a common depth and common focal mechanism. The evidence offered in his paper is not adequate for the evaluation of this claim, but this study shows how sensitive the amplitude ratio is to both factors. Unless changes in relative attenuation are very large, it is unlikely that the velocity structure, focal depth, and focal mechanism will be known well enough to allow their effects to be removed with sufficient accuracy that small Q changes can be isolated.

Acknowledgments

I am grateful to Dr. Jerry P. Eaton (USGS, Menlo Park, California), who kindly provided copies of the Bear Valley film seismograms and the documentation for their use. Dr. Klaus-Peter Bonjer (Geophysical Institute, Karlsruhe University) brought the Darmstadt earthquake to my attention and provided the seismograms, hypocenter solution, and other documentation required for the analysis, as well as for essential background discussions of the Rhine graben earthquakes. This research was supported by the U.S. Geological Survey under Contract 14-08-0001-14581. Mr. Roland LaForge assisted with the calculation of fault plane parameters for the California earthquake. The work was completed while the author was a guest at the Geophysical Institute, Karlsruhe University, under an award from the Alexander von Humboldt Foundation.

References

Bakun, W. H. and C. G. Bufe (1975). Shear wave attenuation along the San Andreas fault zone in central California, *Bull. Seism. Soc. Am.* **65,** 439–459.

Chin, Y., Y. Chao, Y. Chen, C. C. Yen, and Y. J. Cho (1976). A characteristic feature of the dislocation model of the foreshocks of the Haicheng earthquake, Liaoning province, *Acta Geophys. Sinica* **19,** 156–164. Translated in *Chinese Geophysics*, vol. 1, no. 1, T. L. Teng and W. H. K. Lee, Editors, American Geophysical Union, 1978.

Ellsworth, W. L. (1975). Bear Valley, California earthquake sequence of February–March 1972, *Bull. Seism. Soc. Am.* **65,** 483–506.

Engdahl, E. R. and C. Kisslinger (1977). Seismological precursors to a magnitude 5 earthquake in the central Aleutian islands (supplement), *J. Phys. Earth* **25,** 243–250.

Engdahl, E. R. and W. H. K. Lee (1976). Relocation of local earthquakes by seismic ray tracing, *J. Geophys. Res.* **81,** 4400–4406.

Feng, T. Y. (1974). Anomalies of amplitude ratio of S and $\bar{P}$ waves from near earthquakes and earthquake prediction, *Acta Geophys. Sinica* **17,** 140–154. Translated in *Chinese Geophysics*, vol. 1, no. 1, T. L. Teng and W. H. K. Lee, Editors, American Geophysical Union, 1978.

Gutenberg, B. (1944). Energy ratio of reflected and refracted seismic waves, *Bull. Seism. Soc. Am.* **34,** 85–101.

Helmberger, D. V. and L. J. Burdick (1979). Synthetic seismograms, *Ann. Rev. Earth Planet. Sci.* **7,** 417–442.

Kanamori, H. and G. S. Stewart (1976). Mode of the strain release along the Gibbs fracture zone, mid-Atlantic ridge, *Phys. Earth Planet. Interiors* **11,** 312–332.

Landsberg, H. (1931). Der Erdbebenschwarm von Grob-Gerau, 1869–1871, *Gerl. Beitr. z. Geophys.* **34,** 367–392.

Lindh, A., G. Fuis, and C. Mantis (1978). Seismic amplitude measurements suggest foreshocks have different focal mechanisms than aftershocks, *Science* **201,** 56–58.

McEvilly, T. V. and L. R. Johnson (1974). Stability of P and S velocities from central California quarry blasts, *Bull. Seism. Soc. Am.* **64,** 343–353.

McNally, K. C. and T. V. McEvilly (1977). Velocity contrast across the San Andreas fault in southern California: small-scale variations from P-wave nodal plane distortion, *Bull. Seism. Soc. Am.* **67,** 1565–1576.

O'Connell, R. J. and B. Budiansky (1977). Viscoelastic properties of fluid-saturated cracked solids, *J. Geophys. Res.* **82,** 5719–5735.

Stauder, W. (1962). The focal mechanisms of earthquakes, *Adv. Geophys.* **9,** 1–76.

Vvedenskaya, A. V. (1956). Determination of the displacement field of earthquakes by the use of dislocation theory (in Russian), *Izvest. Akad. Nauk S.S.S.R., Ser. Geofiz.*, **3,** 277–284.

Warren, D. H. (1979). Fault-plane solutions for microearthquakes preceding the Thanksgiving day, 1974, earthquake at Hollister, California, *Geophys. Res. Letters* **6,** 633–636.

Wesson, R. L., R. E. Bennett, and K. L. Meagher (1972). Catalog of Earthquakes along the San Andreas Fault System in Central California—January–March 1972, *U.S. Geol. Surv., Open-File Rept.*

Cooperative Institute for Research in Environmental Sciences
University of Colorado
Boulder, Colorado 80309

Manuscript received January 17, 1980